



Thermal Necrosis Assisted Dental Implant Removal: A three-Dimensional Finite Element Analysis

Nayana Prabhu,¹ Krishna Kumar,^{2,*} Ritesh Bhat², Vathsala Patil³, Suhas Kowshik², Utkarsh Swain,^{2,4} Gautam Jaladi^{2,5} and Abhilash Agarwal⁶

Abstract

Dental implants are a common and popular alternative for the replacement of missing teeth. A low degree of regulated thermal necrosis at the bone-implant interface can help avoid the loss of healthy tissue and the risk of damage caused by the removal of the implants. A three-dimension (3D) model of a mandibular section of the bone was used to investigate the optimal contact area required to remove a dental implant via thermal necrosis using a three-dimensional finite element method. The model includes cortical bone, cancellous bone, dental implant, and the crown was created using Dassault Systèmes CATIA V6® product lifecycle management software. Four different contact areas were analyzed by supplying power of 5, 24, and 40 W. At 5 W, the implant temperature is indeterminable for all the three implants considered - Ti6Al4V, titanium dioxide, and zirconia. The results of this investigation showed that increasing the diameter of the contact area not only reduced the time it took for the implant to reach 47°C but also dissipated heat evenly.

Keywords: Dental implant, thermal necrosis, finite element analysis, osseointegration, implant removal, electrocautery.

Received: 14 August 2021; Revised: 12 May 2022; Accepted: 13 May 2022.

Article type: Research article.

1. Introduction

Dental implants are a common and popular alternative for the replacement of missing teeth.^[1,2] The implants are placed in the alveolar bone underneath to offer support for single dental, fastened bridge, or full-arch rehabilitation.^[3] Several complications are usually related to the removal of osseointegrated dental implants that have otherwise failed. The treatment technique is traumatic and frequently results in bone loss.^[4] Several experimental and computational research is conducted to elucidate the mechanism of implant-to-bone load transmission and stress distribution.^[1] Manufacturers have developed different types of implant-abutment

connections to achieve implant stability. However, component (implant) behavior varies based on aspects such as geometry, load circumstances, and implant material properties.^[2,5] Biological factors, such as bacterial plaque subsidence and peri-implantitis, or mechanical factors, such as abutment fracture, implant fracture, screw loosening, and implant displacement, can lead to implant failure after implantation.^[2,4] Implant failures are mainly divided into early failure and late failure as two primary categories. Early failure occurs during the healing process due to poor osseointegration and is physiological and may be due to infection, trauma, and micro-motion of the dental implant.^[5] Treatment suggested for late biological failures is surgical or non-surgical debridement and local antimicrobial therapy.^[5,6] However, the treatment mode prescribed is implant removal for implants that show a radiographic bone loss of more than 50% of their implant body length, mobility, and implants with functional discomfort.^[7] Many underlying tissues, such as nerves, sinuses, palatine bones, and adjacent teeth, maybe damaged when Osseointegrated implants are extracted. The implant cavity typically necessitates an improved bone graft, and a period of 9 to 12 months is required for healing before another implant can be placed. The trauma caused thus leads to delayed treatment schedules, deteriorating the life quality of the patient considerably, and medical expenses for the treatment are

¹ Department of Prosthodontics and Crown & Bridge, Manipal College of Dental Sciences, Manipal, Manipal Academy of Higher Education, Manipal, Karnataka, 576104 India.

² Department of Mechanical and Industrial Engineering, Manipal Institute of Technology, Manipal Academy of Higher Education, Manipal, Karnataka, 576104 India.

³ Department of Oral Medicine and Radiology, Manipal College of Dental Sciences, Manipal, Manipal Academy of Higher Education, Manipal, Karnataka, 576104 India.

⁴ School of Mechanical and Aerospace Engineering, Nanyang Technological University, Nanyang, 707101 Singapore.

*Email: krishna.kumar@manipal.edu (K. Kumar)

exacerbated.^[8,9]

The torque ratchet technique is one of the basic implant removal processes followed by dentists globally. The loss of healthy tissue and trauma can be minimized by weakening the connection between the implant and bone before removal, reducing the force needed for removal. This issue is critical, as the high torque wrench will not easily remove a fairly limited proportion of implants.^[5-7] Several research have demonstrated that, after initial unregulated random thermal therapy, implants can be extracted quickly, resulting in jaw osteonecrosis. A low degree of regulated thermal necrosis at the bone-implant interface can help avoid the loss of healthy tissue and the risk of damage caused by the removal of the implants.^[5-7,9] However, extensive investigations are required to be carried out to study the effects of the rise in temperature at the bone premises and to identify the most favorable conditions for the use of thermal necrosis for a non-traumatic removal of the implant. Also, the relation between the duration of the contact provided and implant size needs to be explored. It has been reported that high-frequency surgical devices and dental lasers have led to peri-implant bone thermal damage, leading to implant failure.^[10] Uncontrolled heating can lead to serious inflammation and necrosis of the jaw.^[11] However, several publications have described the successful loosening of osseointegrated implants using high temperatures with, for example, ultra-high frequency surgical devices.^[12,13] Despite the fact that the heat input in these studies was deliberate, it was uncontrolled and uneven. Nonetheless, this type of implant removal with little thermal necrosis may aid in the preservation of valuable bone tissue during explanations that are challenging. Using the finite element analysis (FEA) method, the present study seeks to determine the best device power, electrocautery tip contact area, and contact duration for inducing deliberate thermal necrosis on an implant system. Three implant materials considered – Ti-6Al-4V, titanium dioxide, and zirconia are subjected to the power of 5, 24, and 40 W to simulate the contact with unipolar electrocautery tips of varied sizes.

2. Experimental

2.1 Materials and methods

A 3D model of a mandibular bone section was utilized in the present study. Wheeler's suggested standard anatomical measurements^[14] served as the foundation for the created

models. The three-dimensional solid model includes cortical bone, cancellous bone, dental implant, and crown. The manufacturer provided the geometry of the dental implant, and the model was created using Dassault Systèmes Catia V6® product lifecycle management (PLM) software. The study was carried out as per the approval of the Institutional Ethics Committee.

2.2 Modeling of the implant

The 3D finite element single-threaded implant with 0.8 mm was constructed using the implant model as a reference, as shown in Fig. 1. The mechanical and thermal properties and restorative materials of the dental structures are defined before the meshing of the solid model. Regardless of its physical properties associated with temperature, the tooth was isotropic, homogenous, and elastic. Table 1 illustrates the elastic properties of these tissues and materials as homogenous, isotropic, and linearly elastic.

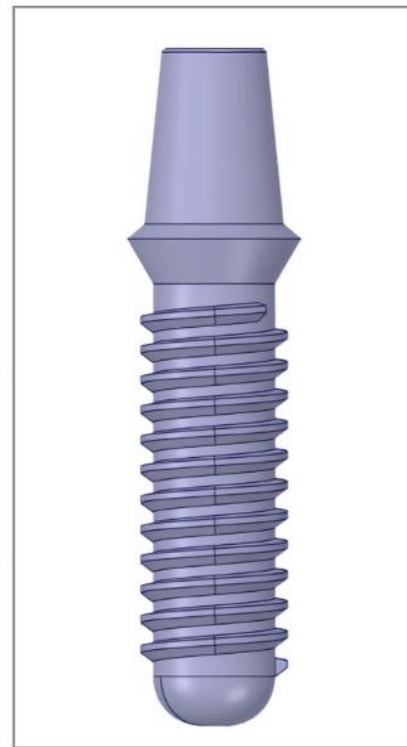


Fig. 1 Modelled implant using Dassault Systèmes CATIA V6 PLM software.

Table 1. Thermal and mechanical properties of the materials used in the FEM model.

	Cortical bone	Trabecular bone	Implant (Ti-6Al-4V)	Implant (titanium dioxide)	Implant (zirconia)
Density (g/cm^3)	1.30	1.30	4.38	4.02	6.04
Thermal conductivity (W/m K)	0.59	0.59	6.52	8	2.7
Specific heat (kJ/kg K)	0.44	0.44	0.57	0.69	0.41

Three types of implant materials were tested, *i.e.*, Ti-6Al-4V, titanium dioxide, and zirconia. The elastic properties of the three materials and the cortical and trabecular bone used in the 3D CATIA models are mentioned in Table 2. A few properties were taken into account when modeling the implant: linear, isotropic, homogeneous, and elastic.

The interfaces between the implant and bone are assumed to undergo complete osseointegration. After the sides and the bottom of the cortical and cancellous/trabecular bones have been fully constrained, the boundary conditions have been applied to the respective node. Components were meshed using tetrahedral meshing with mesh element sizes of 1 mm and a growth rate of 1.5 mm. Figs. 2(a) and 2(b) shows the front view and the isotropic view of the meshed model,

respectively. Fig. 2(c) shows the meshed model of the implant.

Table 2. Material properties of the elements used in the study.

Material	Young's (MPa)	Poisson's ratio
Titanium (Ti-6AL-4V)	1.1×10^5	0.33
Titanium Dioxide (TiO ₂)	2.3×10^5	0.27
Zirconium (Zr)	8.8×10^4	0.30
Cortical Bone	1.5×10^4	0.30
Trabecular Bone	1.5×10^2	0.30

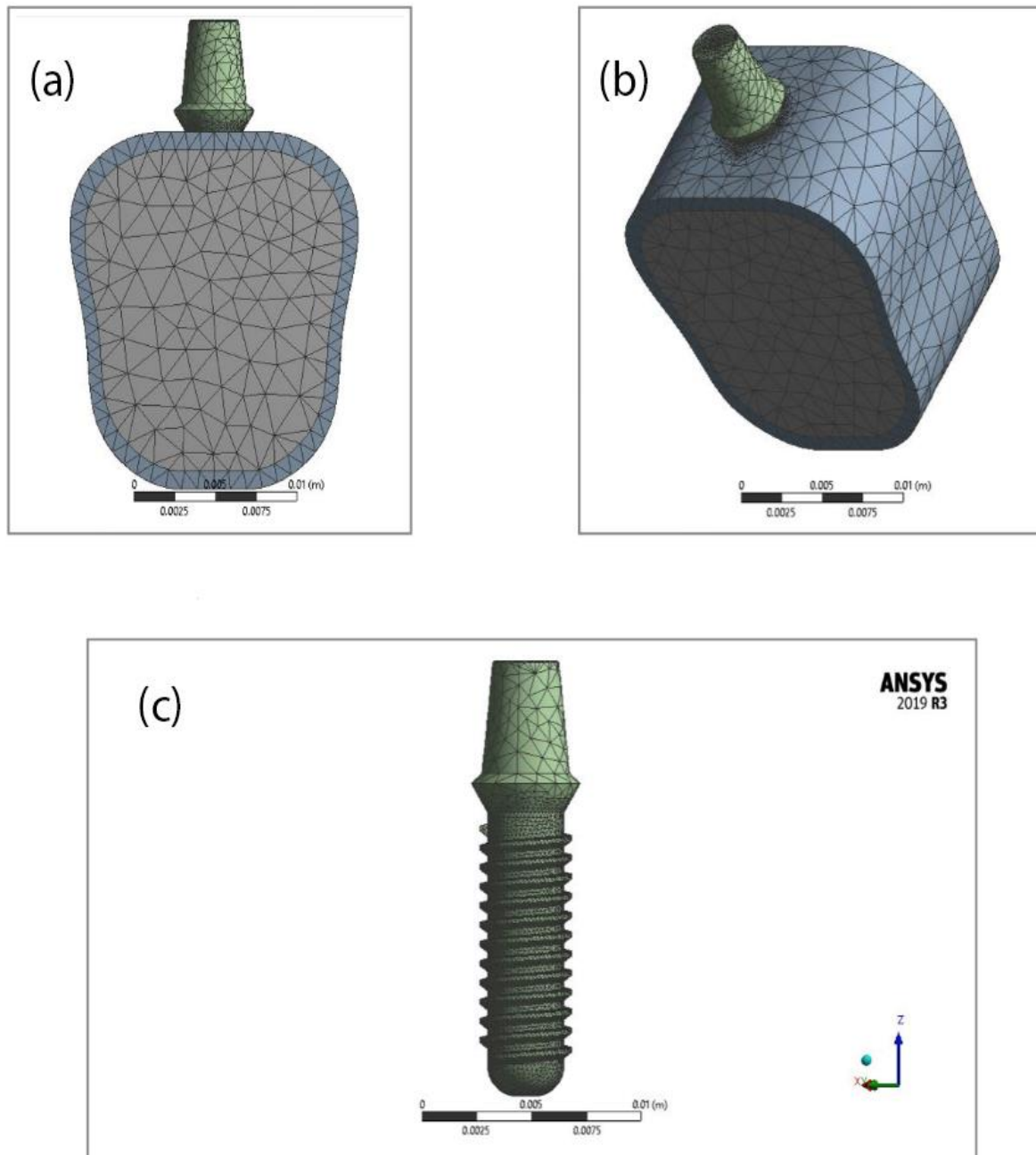


Fig. 2 (a) Front view of the meshed model, (b) isometric view of the meshed model, and (c) meshed model of the implant.

2.3 Finite element conditions

Wang *et al.* recently developed a more detailed three-dimensional FEA model from scanned CT image data. The dimensions of chewing, ligament, and mechanical motion of the temporomandibular joint (TMJ) have been modelled by various components.^[8] Teixeira *et al.* observed that the simulation of the mandible in a 3-dimensional mandibular structure in a mesial or distal gap of more than 4.1 mm from the implant did not lead to a substantial additional yield of FEA precision.^[15]

Defined values of field variables such as relocation and assistance must be imposed on stimulatory model boundaries. Node constraints are established to avoid rotation and changes in either direction. The boundary plays the function of load, *i.e.*, the loading effects are generated by the movement of nodes in a specific direction rather than by the applied forces. In the FEA model, symmetric lines or planes may be described by the perfect symmetrical boundary conditions supplied to geometric edges' symmetric sides. The golden law regarding symmetry is that the vectors perpendicular to the symmetry line are negative and parallel to the axis.^[16,17]

The implants and bones were considered to be at an unvarying temperature of 36 °C during the initial stages of the simulation. This specific temperature was chosen because this is the temperature of the human body. An abrupt rise in the implant temperature was modelled by supplying power of 5, 24, or 40 W, considering four contact areas on the top of the implant device. The transient heat distribution was analysed on the cortical bone, implant, and trabecular bone. A 0.02 second time step was considered during the analysis. The measurements were performed for 4 seconds in total. Time was taken in seconds, and the time required for the cortical bone, implant, and trabecular bone to reach 47 °C was determined. To find the optimal contact area for the implant to reach the designated temperature at the earliest, different circular contact areas were taken up using the diameters of 0.705 mm, 1.41 mm, 2.115 mm, and 2.82 mm. Thus, the contact areas/tip sizes of electrocautery 1.561 mm², 6.245 mm², 14.053 mm², and 24.983 mm² were considered.

3. Results

As the implant-bone was heated to the desired temperature, *i.e.* 47 °C, the implant geometry, and the power output effects were measured.^[18] The time duration given while performing this analysis was nearly equivalent for all the power supplies and contact areas mentioned for the implant and the trabecular bone to be heated to 47 °C.

This is due to the larger contact area between the implant and trabecular bone relative to the region of contact between the cortical bone and the implant. The present study shows an osseointegrated implant undergoing temperature change due to heat supplied at the contact surface of the dental implant using a cautery tip of different sizes with an initial temperature of 36 °C. Temperature change is observed till 4 seconds with a time step of 0.02 seconds. The critical temperature of the

implant is 47 °C, which is critical because the human body can withstand the maximum temperature of 47 °C.^[19] Hence, the time taken to reach 47 °C is noted by applying probes on the implant teeth surface and cortical bone outer surface.

3.1 Titanium dioxide

3.1.1 When 5 W of power is applied

Applying a power of 5 W, the cortical bone reached 47 °C at >4 seconds. Table 3 shows the time taken for a cortical bone and TiO₂ implant to reach 47 °C at 5, 24, and 40 W. The implant surface reached 47 °C at 2.64, 2.64, 2.63, and 2.63 seconds for contact areas of 1.561 mm², 6.245 mm², 14.053 mm², and 24.983 mm², respectively. The temperatures of the implant when the cortical bone reaches 47 °C for the contact areas of 1.561 mm², 6.245 mm², 14.053 mm², and 24.983 mm² are not determinable as the cortical bone does not reach 47 °C within 4 seconds, which was the time limit taken during the iteration.

3.1.2 When 24 W of power is applied

Applying a power of 24 W, the cortical bone reached 47 °C between 3.8-8.82 seconds. The implant surface reached 47 °C at 1.51, 1.51, 1.51, and 1.5 seconds for contact areas of 1.561, 6.245, 14.053, and 24.983 mm². The temperatures of the implant when the cortical bone reaches 47 °C for a contact area of 1.561, 6.245, 14.053, and 24.983 mm² are 151.16, 150.96, 152.05, and 150.29 °C respectively, which are shown in Table 3.

3.1.3 When 40 W of power is applied

Applying a power of 40 W, the cortical bone reached 47 °C between 3.27-3.3 seconds. The implant surface reached 47 °C at 1.3 seconds for contact areas of 1.561, 6.245, 14.053, and 24.983 mm². The temperatures of the implant when the cortical bone reaches 47 °C for a contact area of 1.561, 6.245, 14.053, and 24.983 mm² are 178.8, 178.55, 180.29, and 179.21 °C respectively is shown in Table 3.

3.2 Titanium - Ti-6Al-4V

3.2.1 When 5 W of power is applied

Applying a power of 5 W, the cortical bone reached 47 °C at >4 seconds. Table 4 shows the time taken for a cortical bone and Ti-6Al-4V implant to reach 47 °C at 5, 24, and 40 W. The implant surface reached 47 °C at 2.63, 2.66, 2.66, and 2.66 seconds for contact areas of 1.561, 6.245, 14.053, and 24.983 mm², respectively. The temperatures of the implant when the cortical bone reaches 47 °C for a contact area of 1.561, 6.245, 14.053, and 24.983 mm² is not determinable as the cortical bone does not reach 47 °C within 4 seconds, which was the time limit taken during iteration.

3.2.2 When 24 W of power is applied

Applying a power of 24 W, the cortical bone reached 47 °C between 3.86-3.88 seconds. The implant surface reached 47 °C at 1.56, 1.56, 1.56, 1.55 for contact areas of 1.561, 6.245,

Table 3. Time taken for a cortical bone and TiO₂ implant to reach 47 °C for 5, 24, and 40 W.

Probe (Watts)	Contact area (mm ²)	Time (t) to reach 47°C (sec)		Approx. the temperature of the implant when cortical bone is at 47°C (°C)
		Bone	Implant	
5	1.561	>4	2.64	-
	6.245	>4	2.64	-
	14.035	>4	2.63	47 °C
	24.983	>4	2.63	-
24	1.561	3.82	1.51	151.16
	6.245	3.82	1.51	150.96
	14.035	3.81	1.51	47 °C
	24.983	3.8	1.5	152.05
40	1.561	3.28	1.3	150.29
	6.245	3.28	1.3	178.8
	14.035	3.3	1.3	47 °C
	24.983	3.27	1.3	178.55
				180.29
				179.21

14.053, and 24.983 mm² respectively. The temperatures of the implant when the cortical bone reaches 47 °C for contact areas of 1.561, 6.245, 14.053, and 24.983 mm² are 157.31, 155.9, 157.05, and 156.38 °C, respectively, which are shown in [Table 4](#).

3.2.3 When 40 W of power is applied

Applying a power of 40 W, the cortical bone reached 47 °C between 3.34-3.36 seconds. The implant surface reached 47 °C at 1.35 seconds for contact areas of 1.561, 6.245, 14.053, and 24.983 mm². The temperatures of the implant when the cortical bone reaches 47 °C for contact areas of 1.561, 6.245, 14.053, and 24.983 mm² are 185.31, 36.11, 186.88, and 185.77 °C, respectively, which are shown in [Table 4](#).

3.3 Zirconia

3.3.1 When 5 W of power is applied

Applying a power of 5 W, the surfaces of the implant reached 47 °C at >4 seconds. [Table 5](#) shows the time taken for a cortical bone and Zr implant to reach 47 °C at 5, 24, and 40 W. The implant surface reached 47 °C for more than 4 seconds for contact areas of 1.561, 6.245, 14.053, and 24.983 mm². The temperatures of the implant when the cortical bone reaches 47 °C for a contact area of 1.561, 6.245, 14.053, and 24.983 mm² are not determinable as the cortical bone did not reach 47 °C within 4 seconds, which was the time limit taken during iteration.

3.3.2 When 24 W of power is applied

Applying a power of 24 W, the implant surfaces reached 47 °C in between 3.06-3.08 seconds. The implant surface reached 47 °C at 3.08, 3.08, 3.08, and 3.07 seconds for contact areas of 1.561, 6.245, 14.053, and 24.983 mm², respectively. The temperatures of the implant when the cortical bone reaches 47 °C for a contact area of 1.561, 6.245, 14.053, and 24.983 mm² are not determinable as the cortical bone did not reach 47 °C within 4 seconds, which was the time limit taken during iteration, which is shown in [Table 5](#).

3.3.3 When 40 W of power is applied

Applying a power of 40 W, the implant surfaces reached 47 °C in between 2.72-2.74 seconds. The implant surface reached 47 °C at 2.74, 2.74, 2.74, and 2.72 seconds for contact areas of 1.561, 6.245, 14.053, and 24.983 mm², respectively.

The temperatures of the implant when the cortical bone reaches 47 °C for a contact area of 1.561, 6.245, 14.053, and 24.983 mm² are not determinable as the cortical bone did not reach 47 °C within 4 seconds, which was the time limit taken during iteration, which is shown in [Table 5](#).

4. Discussion

During this analysis, we have studied the variation in temperature resulting from the contact of the electrocautery tip of various tip sizes - 1.561, 6.245, 14.05, and 24.983 mm². These tips sizes/contact areas were analyzed on three different implant materials- Ti-6Al-4V, titanium dioxide, and zirconium

Table 4. Time taken for a cortical bone and Ti-6AL-4V implant to reach 47 °C for 5, 24 and 40 W.

Probe (Watts)	Contact area (mm ²)	Time (t) to reach 47 °C (sec)		Approx. the temperature of the implant when cortical bone is at 47 °C (°C)
		Bone	Implant	
5	1.561	>4	2.63	-
	6.245	>4	2.66	-
	14.053	>4	2.66	47 °C
	24.983	>4	2.66	-
24	1.561	3.87	1.56	157.31
	6.245	3.86	1.56	155.9
	14.053	3.88	1.56	47 °C
	24.983	3.86	1.55	156.38
40	1.561	3.34	1.35	185.31
	6.245	3.34	1.35	185.05
	14.053	3.36	1.35	47 °C
	24.983	3.34	1.35	186.88
				185.77

using FEA. The rise in temperature in a dental implant is usually considered due to various “undesired” consequences such as exposure to hot or cold liquids, laser surgeries, and contact with an electrocautery unit^[10, 18-21] Nevertheless, the conditions in which the temperature is deliberately and controllably increased were investigated in

Table 5. Time taken for a cortical bone and zirconium implant to reach 47 °C for 5, 24 and 40 W.

Probe (Watts)	Contact area (mm ²)	Time (t) to reach 47 °C (sec)		Approx. the temperature of the implant when cortical bone is at 47 °C (°C)
		Bone	Implant	
5	1.561	>4	>4	-
	6.245	>4	>4	-
	14.053	>4	>4	47 °C
	24.983	>4	>4	-
24	1.561	>4	3.08	-
	6.245	>4	3.08	-
	14.053	>4	3.08	47 °C
	24.983	>4	3.07	-
40	1.561	>4	2.74	-
	6.245	>4	2.74	-
	14.053	>4	2.74	47 °C
	24.983	>4	2.72	-

the present research as a technique for facilitating the removal of osseointegrated dental implants or failed implants. To the best of our knowledge, only Wilcox *et al.* [10] have experimentally investigated the increase in temperature of dental implants, an outcome arising from contact with the electrocautery tips. There was an increase in the temperature by 8.87 °C when an electrocautery tip of 5 W came into contact with the implant for 1 second. Figs. 3(a-d) shows the variation of temperature versus time for 5 W with a cautery tip of the contact area of 1.561, 6.245, 14.053, and 24.983 mm² for Ti-6Al-4V, titanium dioxide, and zirconium, respectively.

The results indicate that it is impossible to attain a rise in temperature of 10 °C in the bone as the implant generally reaches higher temperatures while the bone reaches 47 °C. Since the tip sizes were not discussed in the study by Wilcox *et al.*, the tip sizes - 1.561, 6.245, 14.053, and 24.983 mm² were assumed with providing a contact duration of 4 seconds, breaking it down into time steps of 0.02 seconds.[10] In the present study, at 5 W, for all the three implants considered - Ti-6Al-4V, titanium dioxide, and zirconia, the implant temperature is indeterminable, as the bone does not reach

47 °C in the designated contact duration. However, at 24 W, Ti-6Al-4V and titanium dioxide implants reach a temperature range of 150 °C-160 °C when the bone reaches 47 °C. But for zirconia, the bone does not reach 47 °C in the designated contact duration. Figs. 4(a-d) shows the variation of temperature versus time for 24 W with a cautery tip of the contact area of 1.561, 6.245, 14.053, and 24.983 mm² for Ti-6Al-4V, titanium dioxide, and zirconium, respectively.

Finally, at 40 W, Ti-6Al-4V and titanium dioxide implants reach a temperature range of 179-185 °C as the bone reaches 47 °C. In contrast, again, for zirconia implants, the bone does not reach 47 °C in the designated contact duration. For all the computed results, the time to reach 47 °C decreases in small values as the contact area increase due to higher heat dissipation. Figs. 5(a-d) shows the variation of temperature versus time for 40 W with a cautery tip of the contact area of 1.561 mm², 6.245 mm², 14.053 mm², and 24.983 mm² for Ti-6Al-4V, titanium dioxide, and zirconium, respectively. These results imply that the implant material and electrocautery tip sizes are important factors contributing to achieving controlled and limited thermal necrosis.[20] According to a study by

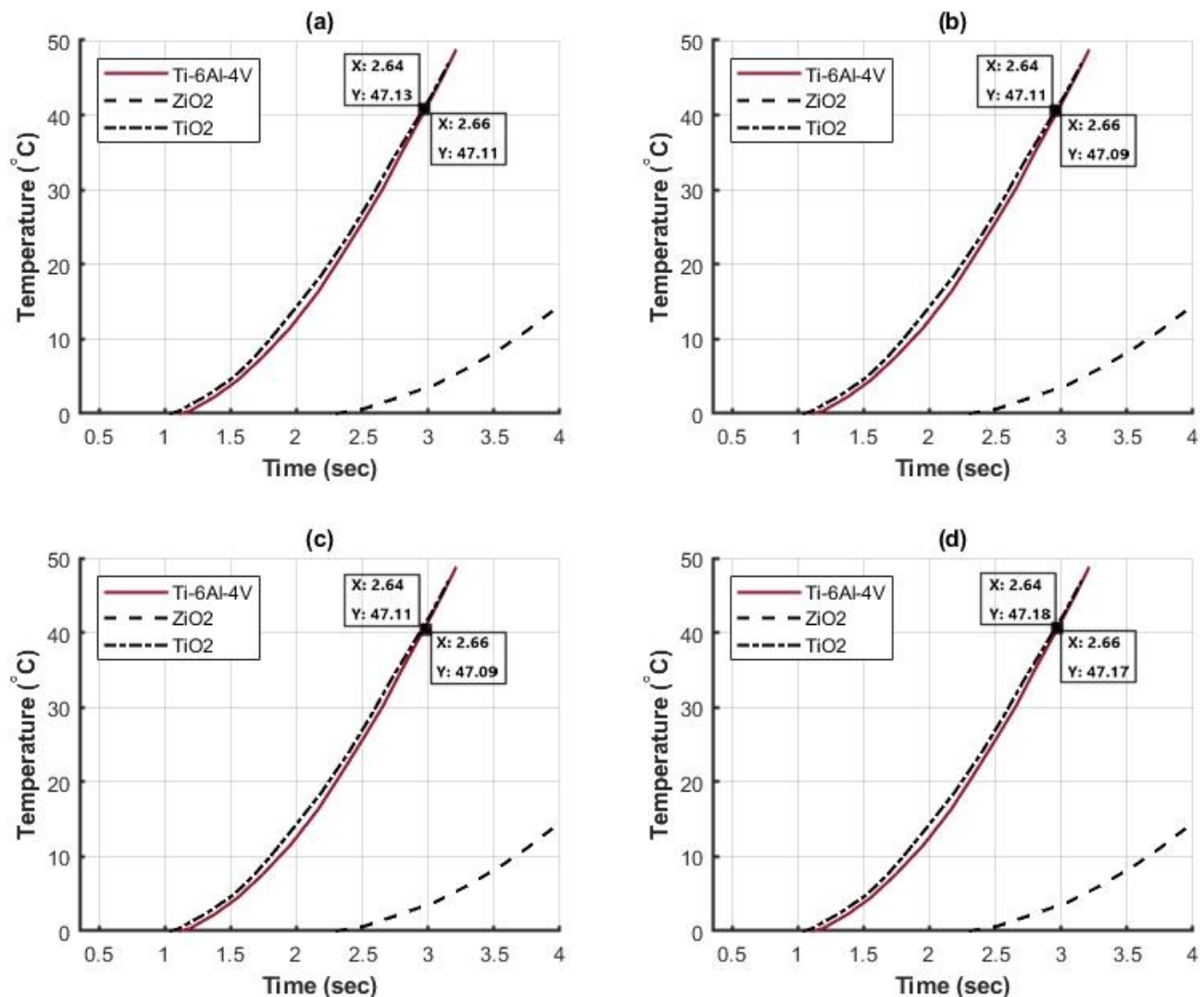


Fig. 3 5 W with a contact area of (a) 1.561 mm² (b) 6.245 mm² (c) 14.053 mm² (d) 24.983 mm².

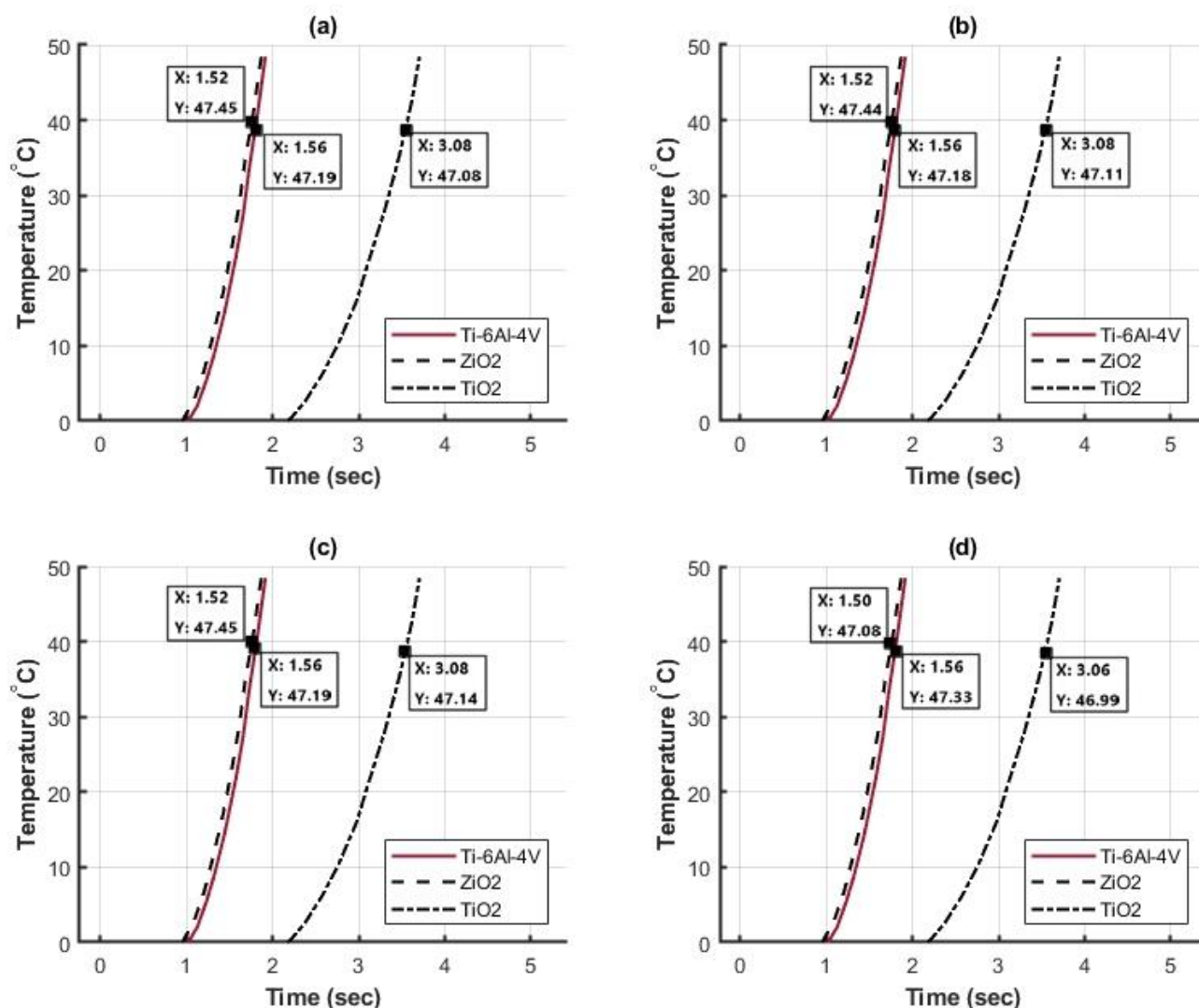


Fig. 4 24 W with a contact area of (a) 1.561 mm² (b) 6.245 mm² (c) 14.053 mm² (d) 24.983 mm².

Mustafa Gungormus *et al.*, the temperature increase of the implants at 40 W power was very rapid; less than 0.5 seconds, and the implants were at unacceptable temperatures as the bone reached 47 °C. Whereas, at 5 W power, a temperature increase of the implants happened at manageable durations, less than 1 second. Furthermore, with larger implants and greater tip diameters, a slower increase in temperature was observed. As a result, for thermal necrosis-aided implant removal, low power settings must be used.

5. Conclusions

The study was conducted to understand better heat transfer in an implant during the removal of osseointegrated implants and reduce complexity during future surgical procedures. The removal of an implant using thermal necrosis is a promising approach for reducing damage and excessive bone loss. This research showed that every brief contact at various power settings leads to a drastic rise in the temperature of implants. In deciding the contact length, the implant and the electrocautery tip contact region were also considered. At 24 W, Ti-6Al-4V and titanium dioxide implants reached a

temperature range of 150 °C-160 °C when the bone reached 47 °C. Concerning zirconia, the bone does not reach 47 °C. At 40 W, Ti-6Al-4V and titanium dioxide implants reached a temperature range of 179-185 °C as the bone reaches 47 °C. In contrast, again, for zirconia, the bone does not reach 47 °C.

Moreover, the results of this investigation also showed that increasing the diameter of the contact area reduced the time it took for the implant to reach 47 °C and dissipated heat evenly.

Acknowledgments

The authors thank the Department of Prosthodontics and Crown & Bridge, Manipal College of Dental Sciences, Manipal and Department of Mechanical and Industrial Engineering, Manipal Institute of Technology for providing the necessary software and lab facilities for the project.

Conflict of Interest

The authors declare no conflict of interest.

Supporting information

Nor applicable.

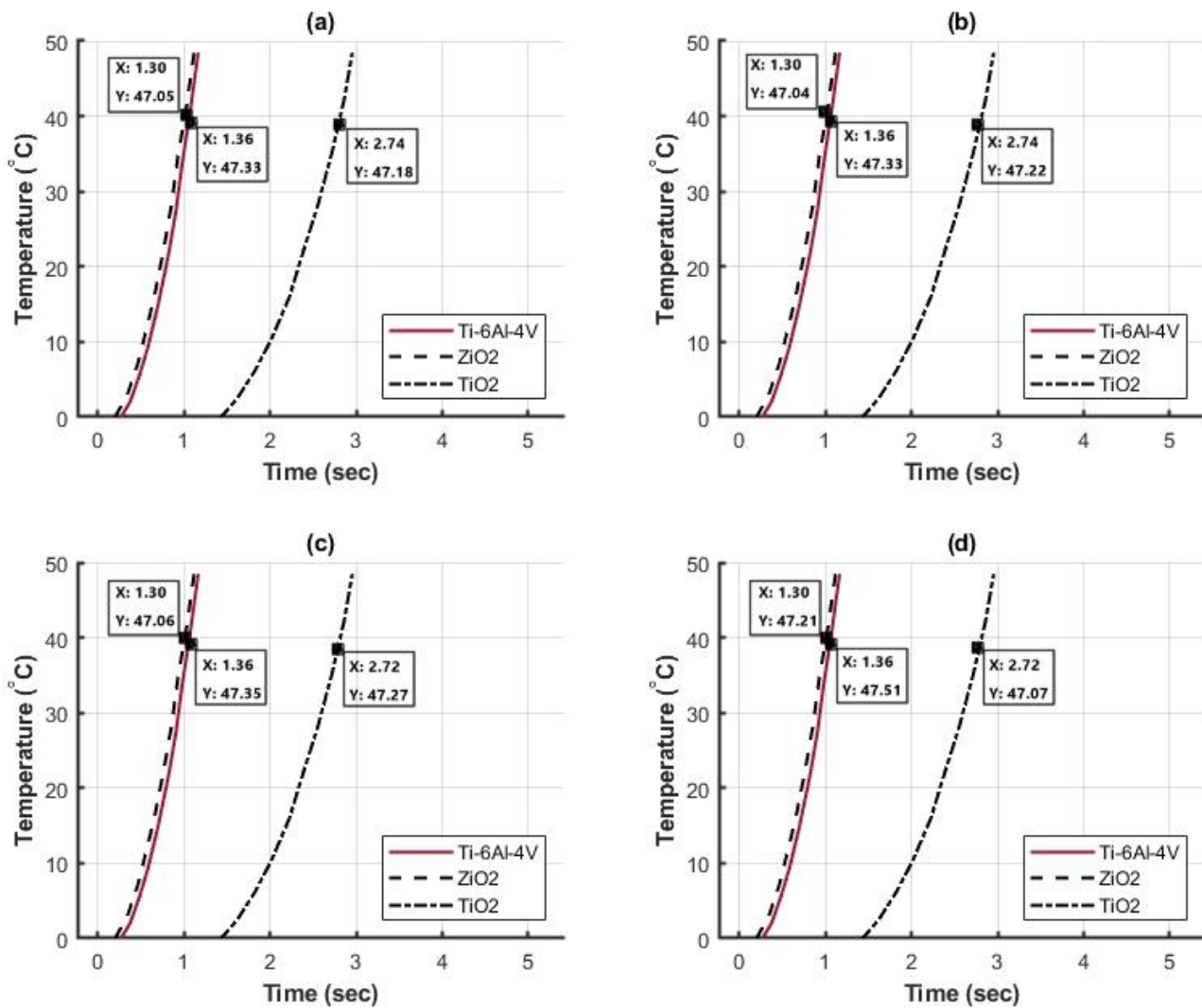


Fig. 5 40 W with a contact area of (a) 1.561 mm² (b) 6.245 mm² (c) 14.053 mm² and (d) 24.983 mm².

Reference

[1] T. W. Koriath, D. P. Romilly, A. G. Hannam, *Am J Phys Anthropol.*, 1992, **88**, 69-96, doi:10.1002/ajpa.1330880107

[2] T. Baiamonte, M. F. Abbate, F. Pizzarello, J. Lozada, and R. James, *J. Oral Implantol.*, 1996, **22**, 104-10.

[3] H.-Y. Chou, J. J. Jagodnik, and S. Muftu, *J. Biomech.*, 2008, **41**, 1365-1373, doi: 10.1016/j.jbiomech.2008.01.032

[4] Z. H. Baqain, W. Y. Moqbel, and F. A. Sawair, *Br. J. Oral Maxillofac. Surg.*, 2012, **50**, 239-243, doi: 10.1016/j.bjoms.2011.04.074.

[5] S. Sakka, K. Baroudi, and M. Z. Nassani, *J. Investig. Clin. Dent.*, 2012, **3**, 258-261, doi: 10.1111/j.2041-1626.2012.00162.x.

[6] Y. Manor, S. Oubaid, O. Mardinger, G. Chaushu, and J. Nissan, *J. Oral Maxillofac. Surg.*, 2009, **67**, 2649-2652, doi: 10.1016/j.joms.2009.07.050.

[7] K. Shemtov-Yona and D. Rittel, *Biomed Res. Int.*, 2015, **2015**, 1-11, doi: 10.1155/2015/547384.

[8] X. D. Wang, X. X. Kou, J. J. Mao, Y. H. Gan, and Y. H. Zhou, *J. Dent. Res.*, 2012, **91**, 499-505, doi: 10.1177/0022034512441946

[9] L. Levin, *Refuat. Hapeh. Vehashinayim.*, 2010, **27**, 6-12, 73, PMID: 20597256.

[10] C. W. Wilcox, T. M. Wilwerding, P. Watson, and J. T. Morris, *Int. J. Oral Maxillofac. Implants*, 2001, **16**, 578-582, doi: 10.1080/09362839109524774.

[11] A. Eriksson, T. Albrektsson, B. Grane, and D. McQueen, *Int. J. Oral Surg.*, 1982, **11**, 115-121, doi: 10.1016/S0300-9785(82)80020-3.

[12] K. Kniha, N. Heussen, E. Weber, S. C. Möhlhenrich, F. Hölzle, A. Modabber, *Materials (Basel)*, 2020, **13**, 3461, 1-14, doi:10.3390/ma13163461

[13] J. Cunliffe and C. Barclay, *J. Dent. Implant.*, 2011, **1**, 22-25, doi: 10.4103/0974-6781.76428.

[14] N. SJ, *Wheeler's Dental Anatomy, Physiology and Occlusion-E-Book*. 2014.

[15] E. R. Teixeira, Y. Sato, Y. Akagawa, and N. Shindoi, *J. Oral Rehabil.*, 1998, **25**, 299-303, doi: 10.1111/j.1365-2842.1998.00244.x.

[16] S. Guven, K. Beydemir, S. Dundar, and V. Eratilla, *Eur. J. Dent.*, 2015, **09**, 329-339, doi: 10.4103/1305-7456.163223.

[17] H. S. Hedia, *J Biomed Mater Res B Appl Biomater.*, 2005, **75**, 74-80, doi:10.1002/jbm.b.30275

- [18] O. Feuerstein, K. Zeichner, C. Imbari, Z. Ormianer, N. Samet, and E. I. Weiss, *Clin. Oral Implants Res.*, 2008, **19**, 629–633, doi: 10.1111/j.1600-0501.2007.01502.x.
- [19] A. Monzavi, S. Shahabi, R. Fekrazad, R. Behruzi, and N. Chiniforush, *J. Dent. (Tehran)*, 2014, **11**, 210–215.
- [20] N. Prabhu, D K Shetty, N Naik, N Shetty, Y Kalpesh Parmar, V Patil and N. Sooriyaperakasam, *Cogent Eng.*, 2021, **8**, doi: 10.1080/23311916.2021.1876582.
- [21] V. Patil, N. Naik, S. Gadicherla, K. Smriti, A. Raju, U. Rathee, *Sci. World J.*, 2020, **2020**, 2363298, doi:10.1155/2020/2363298.

Author Informations



Dr. Nayana Prabhu is Associate Professor in the Department of Prosthodontics and Crown & Bridge and Coordinator of Manipal Implant Program at Manipal College of Dental Sciences, Manipal. She has received her Master's degree from Manipal Academy of Higher Education, in 2006. She has more than 20 years of teaching experience in Dentistry. Her research interest includes the development of Implant surfaces, Dental Materials and Maxillofacial Prosthodontics. She is involved in the academic activities of the Undergraduate and Postgraduate students and guide for Postgraduate dissertation studies. She has guided 7 plus Undergraduate and Postgraduate students in research and project works. She has published several research articles in National and International Journals of repute.



Mr. Krishna Kumar is a faculty of Mechanical and Industrial Engineering at reputed Manipal Institute of Technology, Manipal, a unit of MAHE Manipal. He currently teaches CAD/CAM, FEM to undergraduate students of Mechanical and Industrial engineering. He has academic experience of more than 10 years. He is currently pursuing Ph.D. in the area of Biomechanics of human knee joint. In addition to teaching and learning process he is also the member of UG placement team at the department level. He is also member of department NBA accreditation team. He has also contributed to various student projects as CAD/CAE advisor to CAD/CAE related research. His area of interest includes application of CAD/CAE techniques in the interdisciplinary research area of biomechanics and dental implants.



Mr. Ritesh Bhat is an Assistant Professor (Senior Scale) in the Department of Mechanical and Industrial Engineering at Manipal Institute of Technology, MAHE, Manipal, India. Design of Experiments, Optimization Techniques, Machining of



Dr. Vathsala Patil is currently working as Reader in Department of Oral Medicine and Radiology at Manipal College of Dental Sciences, Manipal. She has BDS degree from SDM College of Dental Sciences, Dharwad, and pursued her MDS degree with the specialization in Oral Medicine and Radiology. She has authored various scientific publications in the area of Dental imaging. She also specializes in management of Oral premalignant and malignant lesions.



Mr. Suhas Kowshik is a Senior Assistant Professor in the department of Mechanical and Industrial Engineering, Manipal Institute of Technology, Manipal, India. He holds B.E.(Mechanical), M.Tech. (Manufacturing Engineering and Technology) and pursuing Ph.D. (composite Materials) degrees. He has more than 8 years in teaching, industry and research experience. His areas of interest include characterization of polymer matrix composites, bio composites and hybrid composites. He has published 14 (Scopus indexed) research papers in reputed international journals and presented 10 research papers in international conferences.



Mr. Utkarsh Swain is presently studying Masters of Science in the field of Mechanical Engineering at Technische Universität Clausthal in Clausthal-Zellerfeld, Germany. He completed his Bachelors in Technology with Honors from Manipal Institute of Technology, India. During the Bachelors he was engaged in a research work under the guidance of Professor in the Mechanical and Industrial Engineering Department. He has a work experience of 1+ years as a Maintenance Engineer. He has leveraged his expertise in manufacturing, design, simulation, testing, and many other facets of the Mechanical engineering discipline at global level.



Mr. Gautam Jaladi currently resides in Florida, USA, and is pursuing his master's degree in industrial and Systems Engineering at Herbert Wertheim College of Engineering, University of Florida. While pursuing his master's degree, he is working part time as an IT Analyst for Enterprise Systems at University of Florida, Information Technology. He obtained his bachelor's degree in Mechanical Engineering from Manipal Institute of Technology, Karnataka. Moreover, four

years of his undergraduate life culminated in a final year capstone project which focused on the biomechanical and thermal studies related to dental implants. He has expertise in using Finite Element Analysis (FEA) on the ANSYS workbench. He has published an article in International journal that discusses the influence of macro and micro designs on the overall performance of a dental implant.



Mr. Abhilash Agarwal currently residing in Singapore is working as an Assistance Field Engineer in TRT Total Risc Technology in Singapore. While being from a small city Jaipur, Rajasthan he completed his under graduation from Manipal Institute of Technology, India where his technical skills and interest lead him to work on research projects. He completed his Masters degree in 2021 from Nanyang Technological University, Singapore where he worked on research project on Natural Ventilation. He is currently working on a project involving designing of medical shoes for flat foot individual. His research interest involves medical solutions, Energy conservation and waste management.

Publisher's Note: Engineered Science Publisher remains neutral with regard to jurisdictional claims in published maps and institutional affiliations.